

LIU Jun¹, QIAN Wei^{1,2,3}, HU Xin¹, AI Xinyu¹ & RAN Xiaojia¹

- ¹ School of Mechanics and Aerospace Engineering, Dalian University of Technology, Dalian 116023, China
- ² State Key Laboratory of Structural Analysis for Industrial Equipment, Dalian University of Technology, Dalian 116023, China
- ³ State Key Laboratory of Structural Analysis for Industrial Equipment, Dalian University of Technology, Dalian 116023, China

Abstract

The high-aspect-ratio wing aircraft has the aerodynamic advantage of low induced drag and becomes the preferred aerodynamic layout for high-altitude long-endurance UAVs. The geometric nonlinear aeroelasticity problem is one of the research hotspots due to the large flexibility of the structure. In this paper, the redistributions of aero pressure, static deformation, and modal frequency, considering geometric nonlinearity, are simulated and analyzed. A subsonic wind tunnel test of a high-aspect-ratio wing is conducted and introduced. An unusual aeroelastic phenomenon occurred in the test, where the deformation of the wing model used gradually decreased before flutter. Besides, the flutter speed in the case of large deformation is bigger. According to the previous simulations, the above two features are well explained. A new mode in which geometric nonlinearity influences the aeroelasticity of high-aspect-ratio wings is investigated and summarized.

Keywords: High-aspect-ratio; Aeroelasticity; Geometric nonlinearity; Wind tunnel test

1. Introduction

Many studies have focused on high-aspect-ratio wings for advancements in aircraft design due to the high lift-drag ratio and resulting improvements in fuel efficiency[1–3]. It is widely used in high-altitude, long-endurance aircraft.

The large flexibility of high-aspect-ratio wings has an essential influence on aircraft structural design and optimization. Maxwell Blair et al. presented an integrated process that advances the design of an aeroelastic joined-wing concept by incorporating physics-based results at the system level[4]. D. E. Calderon et al. used a nonlinear finite element beam model that adopted the finite volumes concept with an intrinsic strain and curvature formulation to size a single-aisle passenger aircraft[5]. Eirikur Jonsson et al. from the University of Michigan developed a framework integrating a geometrically nonlinear flutter constraint, which considers in-flight deflections, into a high-fidelity gradient-based aero-structural optimization[6,7].

Research on the aeroelasticity of high-aspect-ratio wing UAVs has become very popular in recent years. Alvaro Cea and Rafael Palacios studied the aeroelastic response of a long-range aircraft. They emphasized the difference between linear and nonlinear approaches in calculating the aircraft flying equilibrium, dynamic perturbations, and variations to the flutter boundary[8]. R. G. Cook et al. analyzed the gust load response of a high-aspect-ratio aircraft, considering the effect of geometric nonlinearity[9]. Hanif S. Hoseini and Dewey H. Hodges conducted linear and nonlinear divergence and flutter analysis on damaged high-aspect-ratio composite wings with large deformation[10].

Simulation and wind tunnel tests were conducted to study the aeroelasticity of high-aspect-ratio wings. The paper is organized as follows. Section 2 describes the aero pressure distribution simulation of high-aspect-ratio wings. Section 3 introduces the modal analysis with geometric nonlinearity of the baseline wing. Section 4 presents details of the wind tunnel test phenomenon. Conclusions are drawn in section 6.

2. Redistributions of Aero Pressure

A representative model of a high-aspect-ratio wing is used to study the distribution of pressure centers. The wing consists of skins, a single beam, and ribs. It is 4000mm spanwise and 400mm chordwise (see Figure 1). Figure 2 shows the model built in MSC Nastran. Solution 144 of MSC Nastran is conducted to calculate the lift force of the aerodynamic model. Interpolation points are selected from all nodes of the suction surface of the wing finite element model. The lift force obtained is assumed to be concentrated uniformly across the one-quarter chord line of each box. According to the definition of pressure center, the pitch moment about the pressure center in each airfoil section is zero. Therefore, the location of the pressure center is calculated chordwise (see Figure 3).

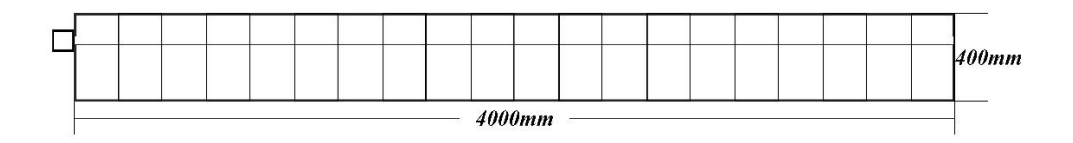


Figure 1 – Geometric information of the wing model.

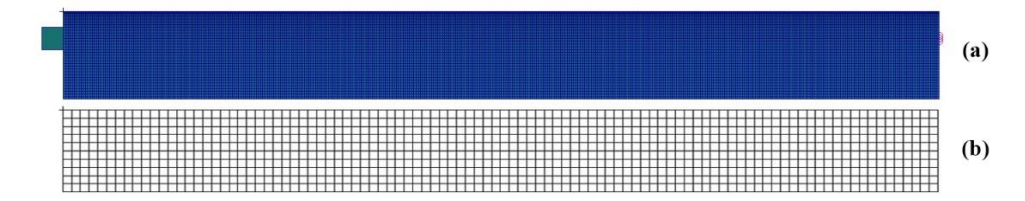


Figure 2 – Simulation models in MSC Nastran: (a) wing structure FEM; (b) aerodynamic boxes.

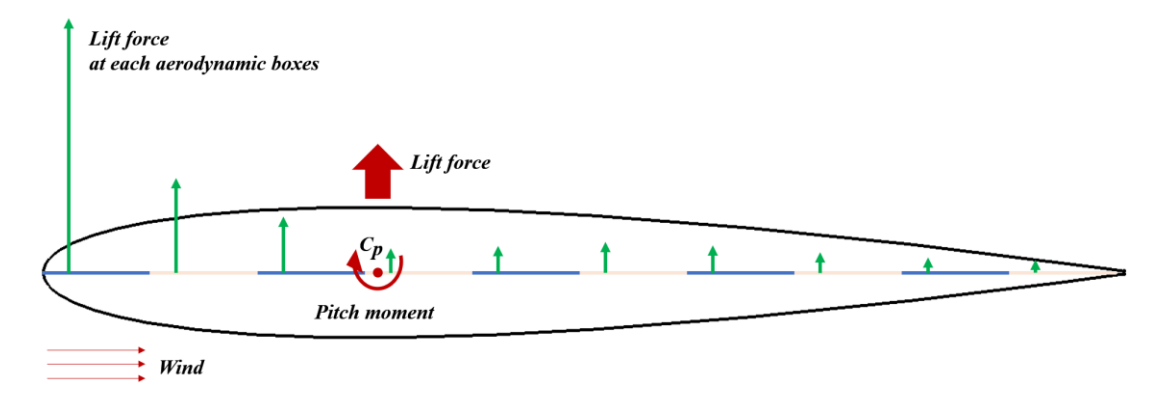


Figure 3 – Definition of Cp in each cross-section.

Two variables are studied: the wind speed and the stiffness of the skin. As for the baseline model, Young's modulus of skin is 500MPa, and the location of CP is calculated with the 5-degree angle of attack (AoA). The wind speed varies from 10m/s to 20m/s, and the distribution of CP spanwise and chordwise is shown in Figure 4. As the wind speed increases, the CP moves toward the trailing edge. Besides, the curve of each wind speed is wave-shaped, and the number of peaks is equal to the number of wing boxes. This is because the wing stiffness distribution is not uniform spanwise due to the influence of the wing ribs. However, the movement of CP is more evident in the section without wing ribs.

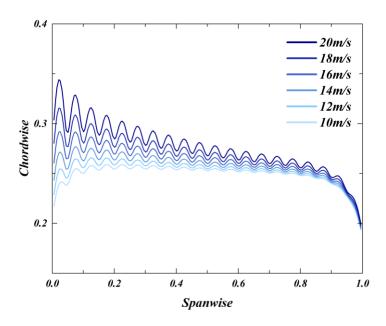


Figure 4 – Distribution of CP spanwise and chordwise at different wind speeds of the baseline model (500MPa).

The Young's modulus of skin is increased to 10000MPa, and the CP distribution is shown in Figure 5. It has the same behavior as the baseline model. However, the movement of the CP chordwise is much smaller, which means there is nearly no movement.

To further investigate the effect of stiffness on the position of CP, several extra calculations are conducted at a wind speed of 12m/s and a 5-degree AoA. Figure 6 shows that the distance the CP moves chordwise increases as the skin stiffness decreases. In summary, the chordwise pressure distribution changes significantly for wings with less stiffness in the wing skin, which is caused by static aeroelasticity.

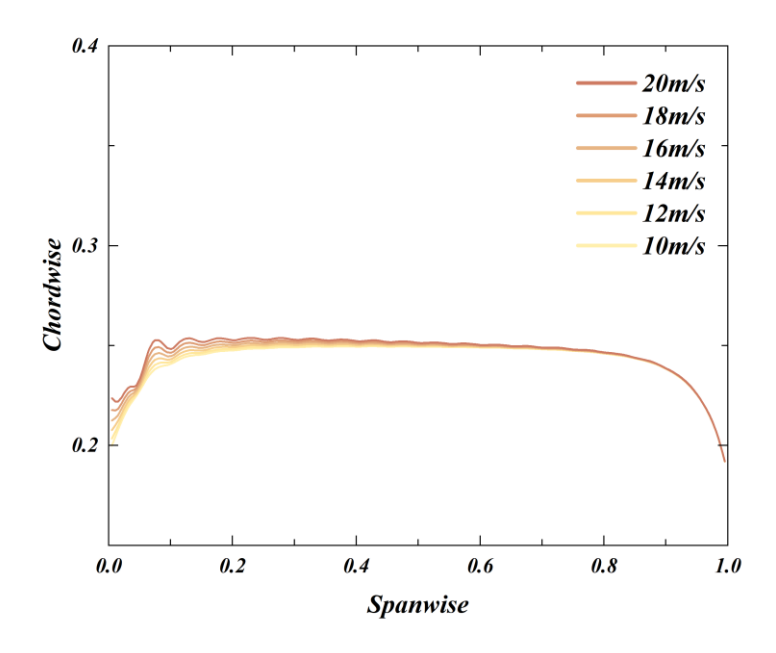


Figure 5 – Distribution of CP spanwise and chordwise at different wind speeds of the large stiffness model (10000MPa).

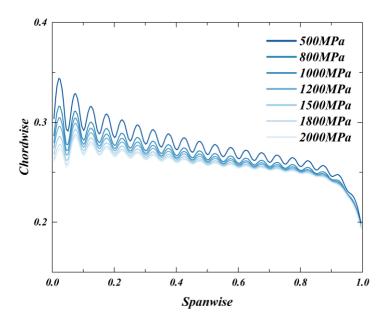


Figure 6 – Distribution of CP spanwise and chordwise of different skin stiffness models at 12m/s wind speed and 5-degree AoA.

3. Static and Modal Analysis with Geometric Nonlinearity

Geometrically nonlinear static analysis of the baseline model uses solution 106 of MSC Nastran. The aerodynamic forces on each section, obtained by solution 144, are equated to the aerodynamic lift and pitch moments acting at the location of the main beam of the section (see Figure 7). As shown in Figures 8 and 9, the deformation of nonlinear analysis is less than that of linear analysis. As the load increases, the trend of deformation slows down. Besides, the nonlinear effect becomes more apparent with higher wind speeds.

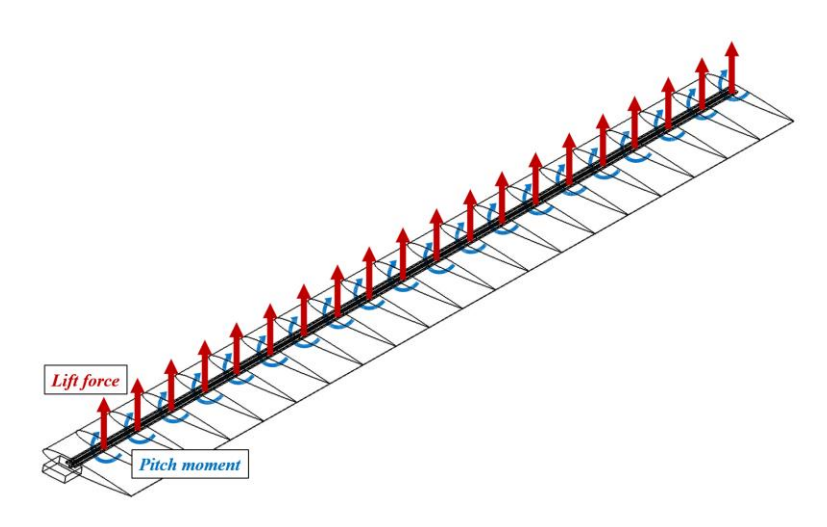


Figure 7 – Equivalent aerodynamic forces and moments in cross-sections.

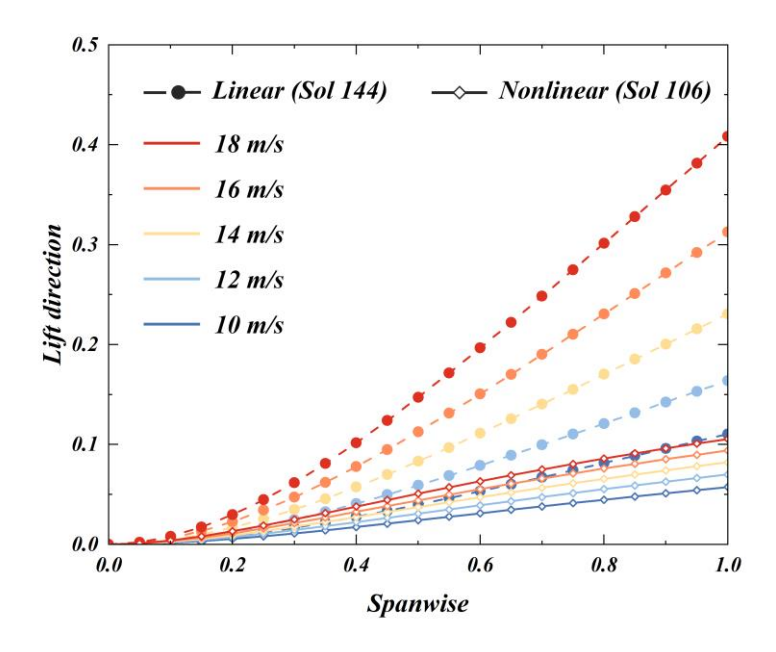


Figure 8 – Linear and nonlinear deformations along the span direction at different wind speeds.

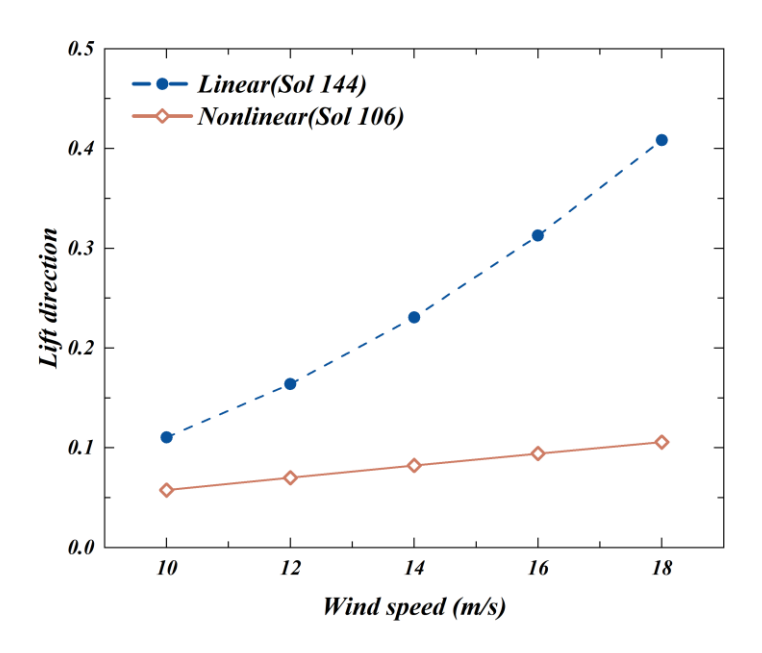


Figure 9 – Linear and nonlinear deformations of the wing tip at different wind speeds.

The modes of the baseline model under the aerodynamic loads are calculated using solution 106. With the deformation increases in the lift direction, the stiffness of the wing also changes. As shown in Figure 10, the torsion modal frequency is very sensitive to deformation in the lift direction. And it is positively correlated with deformation. The out-plane bending modal frequencies also increase with deformation growing, but the rate of increase is significantly smaller than that of the torsional mode. The in-plane bending modal frequencies are unaffected by deformation.

Since the wing flutter speed is closely related to the structural modes, it can be hypothesized that the changes in the structural modes must significantly impact the flutter critical speed due to the geometrical nonlinearities.

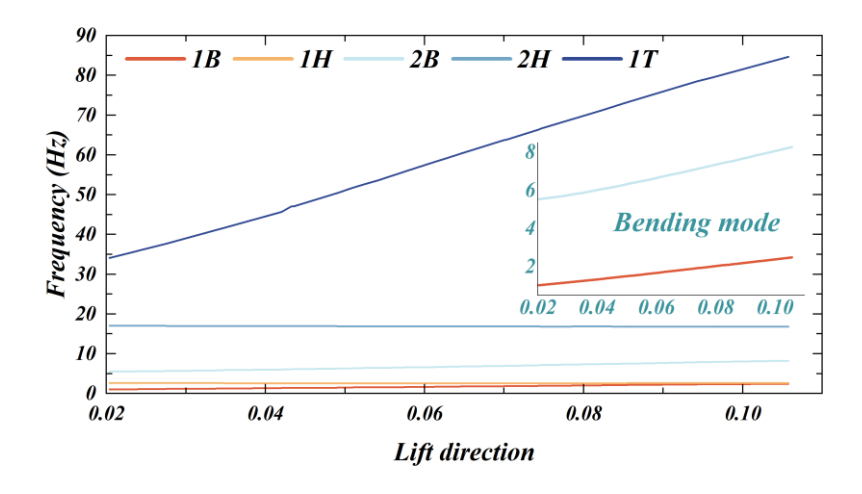


Figure 10 – Variations of modal frequencies as deformation increases.

4. Wind Tunnel Tests of A High-aspect-ratio Wing

The primary objective of the test campaign is to estimate the geometric nonlinearity effects on the flutter phenomena of the high-aspect-ratio wing. The experimental tests campaign has been performed in a subsonic wind tunnel facility. It is a closed circuit tunnel with a rectangular cross-section and tempered edges. The model is 4500mm spanwise and about 450mm chordwise, which was mounted on the wind tunnel ceiling during the test. Two acceleration sensors were mounted on the leading and trailing edges of the wingtip.

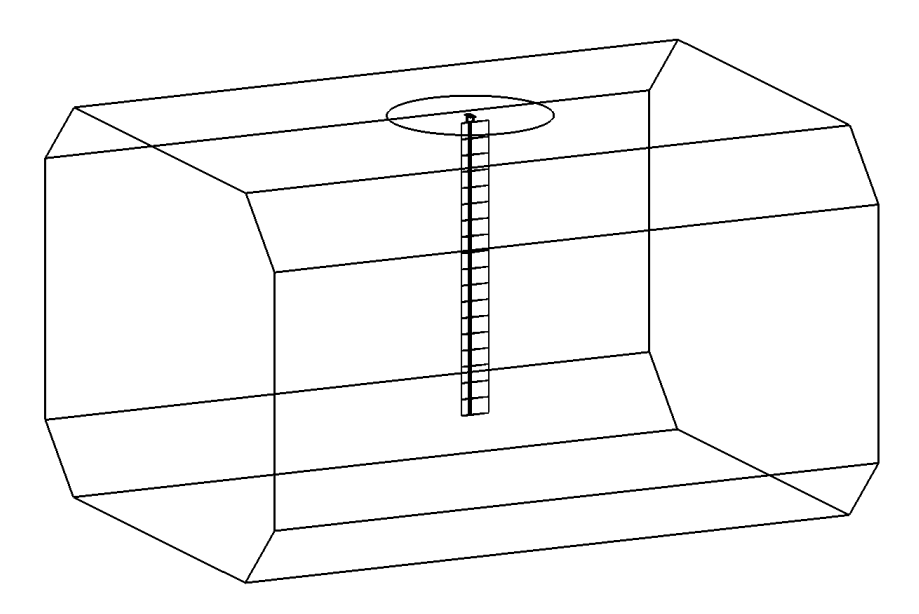


Figure 11 – Model installation in the wind tunnel.

The test was conducted at a fixed AoA with variable wind speeds. Two prominent test cases are introduced here.

Case 1: the model is mounted at a zero-lift AoA.

The acceleration responses at the zero-lift AoA are shown in Figure 12 (a). Table 1 lists the wind speed steps during case 1. Responses of the last four wind speeds are extracted and shown in Figure 13 (a). The vibration response amplitude increases dramatically when the wind speed increases to 16.2m/s. The wing vibrates violently, accompanied by apparent equal amplitude oscillation when the flutter phenomenon occurs. As the wind speed increases, a single spectrogram peak appears in the low-frequency range, and the flutter frequency is 6.3Hz, see Figure 14 (a).

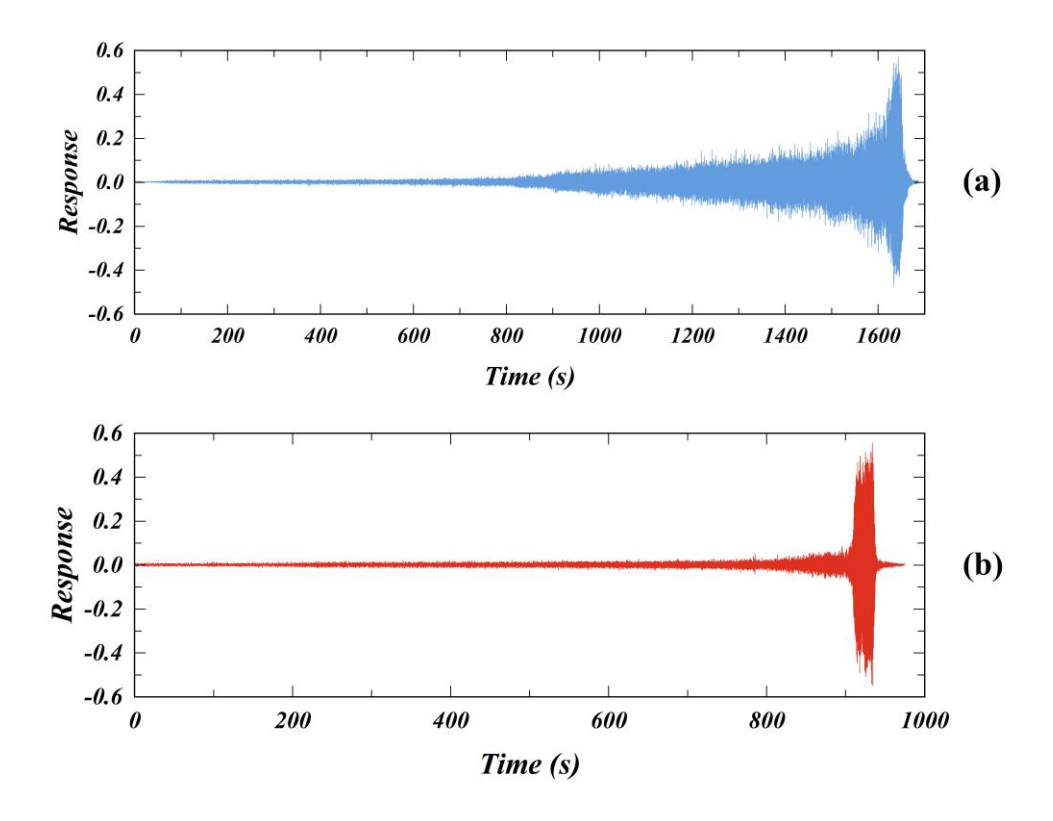


Figure 12 – The acceleration responses at the zero-lift AoA: (a) case 1; (b) case 2.

Table 1 – Wind speed steps in test case 1.

Steps	Wind speed (m/s)
1	8.0
2	9.0
3	10.0
4	11.0
5	12.0
6	12.5
7	13.0
8	13.5
9	14.0
10	14.5
11	15.0
12	15.5
13	16.0
14	16.2

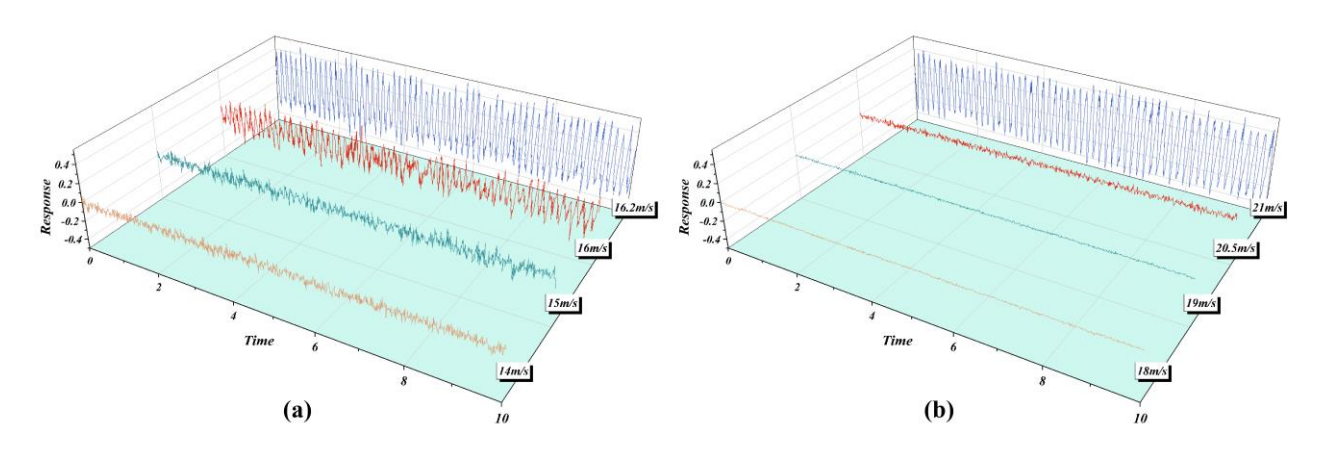


Figure 13 – Responses of the last four wind speeds: (a) case 1; (b) case 2.

Case 2: the AoA is increased by 4 degrees from case 1.

The wind speeds of test case 2 are listed in Table 2. Figure 12 (b) presents the responses of the wing tip during the test case 2. In this test case, an unusual phenomenon occurs. The deformation in the lift direction increases in the low wind speed range. When the wind speed reaches some value, the deformation does not continue to grow but moves in the opposite direction. Besides, when the wind speed increases to the flutter wind speed in case 1, in which the wing has no deformation, the flutter phenomenon does not occur. The equal-amplitude oscillation phenomenon occurs as the wing deformation decreases and approaches the zero-deformation state. The flutter speed is 21.0m/s (Figure 13 (b)), and the frequency is 5.7Hz (Figure 14 (b)).

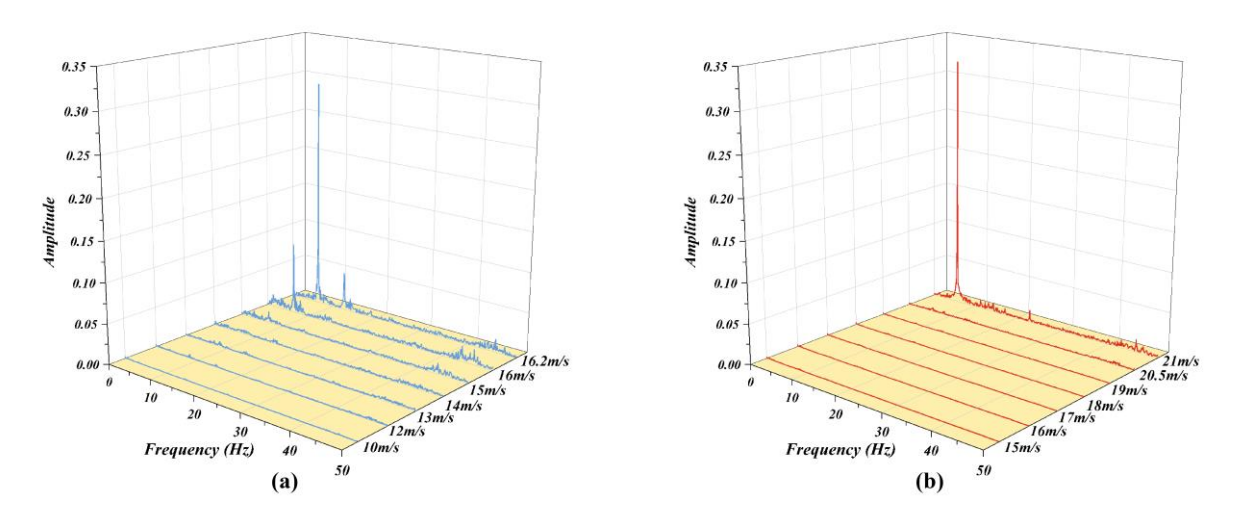


Figure 14 – Spectrogram at different wind speeds: (a) case 1; (b) case 2.

Table 2 – Wind speed steps in test case 2.

Table 2 – Willia speed steps in test case 2.	
Steps	Wind speed (m/s)
1	8.0
2	10.0
3	12.0
4	14.0
5	15.0
6	16.0
7	17.0
8	17.5
9	18.0
10	18.5
11	19.0
12	19.5
13	20.0
14	20.5
15	21.0

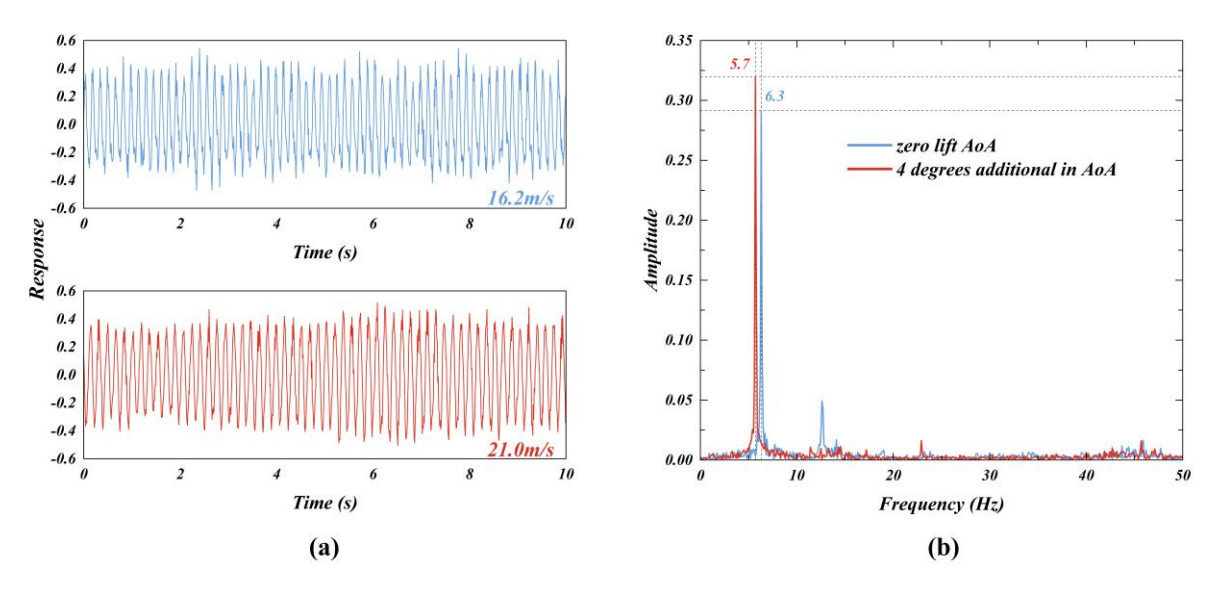


Figure 15 – The comparisons of response and spectrogram at flutter speed between cases 1 and 2.

The comparisons of response and spectrogram at flutter speed between case 1 and case 2 are shown in Figure 15. From the above two test cases, there are two apparent features.

Firstly, at the AoA in case 2, the wing deformation does not increase all the time but appears to increase and decrease under large wind speeds, and flutter occurs at a state close to zero deformation. According to the former analysis, the deformation increases as the wind speed grows until it reaches a particular position due to geometric nonlinearity. Considering the low Young's modulus of skin, the wing load distribution will change more significantly. As the aerodynamic loads increase, the pressure loads are redistributed, and the CP moves toward the trailing edge, resulting in a reduced or possibly even negative pitching moment. The local AoA of the wing is small or even reversed. Under the joint action of the structural elastic restoring force and the large gravity component brought about by the large deformation, the deformation reduction occurs until it tends to the state where the deformation is zero.

Secondly, large deformation of the wing delays the flutter. Based on the analysis of the influence of deformation on the wing modes, it can be inferred that the flutter is delayed due to the change in the structural modes. Because of the deformation rebound phenomenon, the geometric nonlinear effects are weakened when the wing is restored to a near-zero deformation state, and at this time, due to the smaller structural deformation. The wing modes are restored to the state with nearly no deformation, and the flutter occurs.

5. Conclusions

In this study, the relationship between the position of CP with wind speed and the skin stiffness for a high-aspect-ratio wing is simulated. The regularity of modes and frequency under large deformation is investigated through geometric nonlinear static calculation and modal analysis. Besides, the phenomena of deformation rebound and increased flutter speed during the wind tunnel test were successfully explained.

This study illustrates that for a high-aspect-ratio wing model with low skin stiffness, the aerodynamic loads will be redistributed, and the deformation will be reduced under the combined effect of geometric nonlinearity and static aeroelasticity. The phenomenon can even further affect the aeroelastic response.

Although skin materials with such low stiffness are generally not used in the design process of high-aspect-ratio airplanes. However, they are widely used in designing subsonic wind tunnel test models to ensure the accurate design of mass and stiffness. Therefore, skin stiffness should be emphasized during the design of the high-aspect-ratio wing WTT model.

Further research will be conducted to support the conclusions of this paper.

- a) Tests of mode shapes and frequencies under different wind speeds (different deformations).
- b) Wind tunnel tests of high-aspect-ratio wings with variable skin stiffness to investigate the reason for deformation reduction.

6. Contact Author Email Address

The contact author email address is: qianwei@dlut.edu.cn

7. Copyright Statement

The authors confirm that they, and/or their company or organization, hold copyright on all of the original material included in this paper. The authors also confirm that they have obtained permission, from the copyright holder of any third party material included in this paper, to publish it as part of their paper. The authors confirm that they give permission, or have obtained permission from the copyright holder of this paper, for the publication and distribution of this paper as part of the ICAS proceedings or as individual off-prints from the proceedings.

References

- [1] Banneheka Navaratna, P.D.; Pontillo, A.; Rezgui, D.; Lowenberg, M.H.; Neild, S.A.; Cooper, J.E. Design and Assessment of Subscale Flexible High Aspect Ratio Cantilever Wings. In Proceedings of the AIAA SciTech 2022 Forum; American Institute of Aeronautics and Astronautics: San Diego, CA & Virtual, January 3, 2022.
- [2] Patil, M.J.; Hodges, D.H.; Cesnik, C.E.S. Nonlinear Aeroelasticity and Flight Dynamics of High-Altitude Long-Endurance Aircraft. Journal of Aircraft 2001, 38, 88–94, doi:10.2514/2.2738.
- [3] Patil, M.J.; Hodges, D.H. On the Importance of Aerodynamic and Structural Geometrical Nonlinearities in Aeroelastic Behavior of High-Aspect-Ratio Wings. Journal of Fluids and Structures 2004, 19, 905–915, doi:10.1016/j.jfluidstructs.2004.04.012.
- [4] Blair, M.; Canfield, R.A.; Roberts, R.W. Joined-Wing Aeroelastic Design with Geometric Nonlinearity. Journal of Aircraft 2005, 42, 832–848, doi:10.2514/1.2199.
- [5] Calderon, D.E.; Cooper, J.E.; Lowenberg, M.; Neild, S.A.; Coetzee, E.B. Sizing High-Aspect-Ratio Wings with a Geometrically Nonlinear Beam Model. Journal of Aircraft 2019, 56, 1455–1470, doi:10.2514/1.C035296.
- [6] Gray, A.C.; Riso, C.; Jonsson, E.; Martins, J.R.R.A.; Cesnik, C.E.S. High-Fidelity Aerostructural Optimization with a Geometrically Nonlinear Flutter Constraint. AIAA Journal 2023, 61, 2430–2443, doi:10.2514/1.J062127.
- [7] Jonsson, E.; Riso, C.; Monteiro, B.B.; Gray, A.C.; Martins, J.R.R.A.; Cesnik, C.E.S. High-Fidelity Gradient-Based Wing Structural Optimization Including Geometrically Nonlinear Flutter Constraint. AIAA Journal 2023, 61, 3045–3061, doi:10.2514/1.J061575.
- [8] Cea, A.; Palacios, R. Geometrically Nonlinear Effects on the Aeroelastic Response of a Transport Aircraft Configuration. Journal of Aircraft 2023, 60, 205–220, doi:10.2514/1.C036740.
- [9] Cook, R.G.; Calderon, D.E.; Cooper, J.E.; Lowenberg, M.H.; Neild, S.A. Industrially Inspired Gust Loads Analysis of Various-Aspect-Ratio Wings Featuring Geometric Nonlinearity. Journal of Aircraft 2020, 57, 13–28, doi:10.2514/1.C035294.
- [10] Hoseini, H.S.; Hodges, D.H. Aeroelastic Stability Analysis of Damaged High-Aspect-Ratio Composite Wings. Journal of Aircraft 2019, 56, 1794–1808, doi:10.2514/1.C035098.